Nature of the Transition Metal−Cycloheptatrienyl Bond. Computational Studies of the Electronic Structure of [M(η^7-C_7H_7)(η^5-C_5H_5)] (M = groups 4−6)

Giuseppina Menconi and Nikolas Kaltsoyannis*

Department of Chemistry, University College London, 20 Gordon Street, London WC1H 0AJ, U.K.

Received September 28, 2004

The geometric and electronic structures of the title compounds are investigated using relativistic, gradient-corrected density functional theory. The metal−ligand bond lengths in the transactinide compounds are found to be generally larger than for the 3d, 4d, and 5d systems, suggesting that the actinide contraction is not significantly bigger than the lanthanide analogue. Excellent agreement is obtained between computed and experimental valence ionization energies. The localization properties of the key $1e_2$ electrons are analyzed and suggest that the cycloheptatrienyl ring functions more as a −3 ligand than as a +1 ligand in these mixed ring complexes. Comparisons are made with previous photoelectron spectroscopic determinations of the character of the $1e_2$ electrons. The metal−cycloheptatrienyl bonding energies are calculated and are found to be weakest for the transactinide molecules.

Introduction

Hückel tells us that, in order for a planar carbocyclic ring of general formula C_mH_m to be aromatic, it must possess $4n+2$ pπ electrons, where $n = 0, 1, 2, ...$[1] The two most commonly encountered carbocyclic ligands in organometallic chemistry—the cyclopentadienyl (cp) monoanion and neutral benzene (bz)—both possess six such pπ electrons (in a closed-shell arrangement). The oxidation state of the metal generated by cp^- and bz in their complexes is unambiguous.

For cycloheptatrienyl (cht), η^7-C_7H_7, the situation is less clear-cut, as the neutral molecule possesses seven pπ electrons with a single electron in a doubly degenerate e_2'' symmetry (D_{7h}) highest occupied molecular orbital (HOMO). Thus both a +1 and a −3 formal charge satisfy the Hückel $4n+2$ rule (respectively corresponding to removal of the single e_2'' electron and filling of the e_2'' levels), raising interesting questions of electron localization and metal oxidation state assignment.

More than a decade ago, one of us was involved in experimental studies of the nature of the bonding between the transition metal and the cht ring in complexes of the form [M(η^7-C_7H_7)(η^5-C_5H_5)], where M was drawn from groups 4−6 of the periodic table.[2,3] These experiments employed both discharge lamp and synchrotron radiation-based photoelectron spectroscopy and determined the variation of photoelectron band cross sections with the energy of the ionizing radiation. The bands due to metal-localized electrons show cross section variations quite distinct from those of carbon p-based electrons, and comparison of these variations allowed detailed conclusions to be drawn concerning the nature of the early transition metal−cht bond. These conclusions are best understood with reference to Figure 1, a qualitative valence MO scheme for a transition metal in the pseudoaxial ligand field generated by the cht and cp ligands, in which only the interaction of the e symmetry pπ MOs of the ligands with the metal d orbitals is considered. The metal d orbitals split into three sets, as indicated in Figure 1, which are of σ ($1a_1 - d_{z^2}$), π ($3e_1 - d_{xz}, d_{yz}$), and δ ($1e_2 - d_{x^2-y^2}, d_{xy}$) symmetry with respect to the metal−ring centroid axes (assuming infinite axes of rotation for the carbocyclic rings allows us to treat the electronic structure within the $C_{\infty v}$ point group). The highest occupied MO in 16-electron group 4 systems is the $1e_2$ level, while the group 5 and group 6 molecules have 1 and 2 electrons, respectively, in the $1a_1$ MO.

The synchrotron study revealed that the electrons in the $1e_1$ and $2e_1$ MOs of [M(η^7-C_7H_7)(η^5-C_5H_5)] (M = Ti, Nb, Mo) and [Ta(η^7-C_7H_7)(η^5-C_5H_4Me)] are predominantly carbon p-based.[3] The cross sections of the electrons in the $1a_1$ MO of the group 5 and group 6 systems, however, display features characteristic of d-based electrons, most notably p → d giant resonances in the energetic vicinity of the semi-core np ionizations. The cross section variations of the $1e_2$ electrons of the group 5 and group 6 molecules were found to be intermediate between those of the d-based $1a_1$ electrons and the carbon p-based $2e_1$ and $1e_1$ electrons. The conclusion was therefore that the $1e_2$ electrons contain significant contributions from both the metal d and the ligand pπ orbitals. More quantitatively, the $1e_2$ MOs of [Nb(η^7-C_7H_7)(η^5-C_5H_5)] and [Mo(η^7-C_7H_7)(η^5-C_5H_5)] were estimated to be 63% metal d in character, while the

* To whom correspondence should be addressed. E-mail: n.kaltsoyannis@ucl.ac.uk.

(1) Hückel, E. *Z. Phys.* **1932**, *76*, 628.
(2) Green, J. C.; Green, M. L. H.; Kaltsoyannis, N.; Mountford, P.; Scott, P.; Simpson, S. J. *Organometallics* **1992**, *11*, 3353.
(3) Green, J. C.; Kaltsoyannis, N.; MacDonald, M. A.; Sze, K. H. *J. Am. Chem. Soc.* **1994**, *116*, 1994.

10.1021/om0492505 CCC: $30.25
Publication on Web 02/09/2005

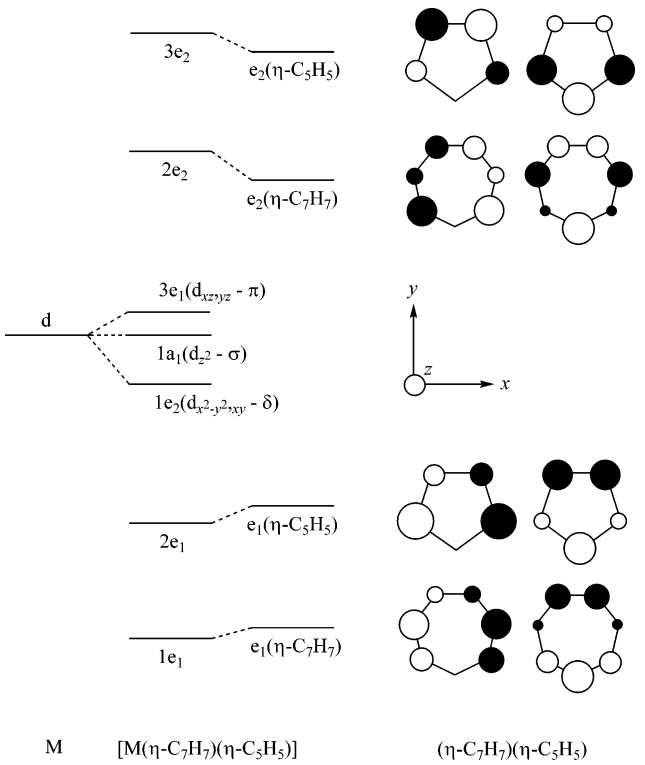

Figure 1. Qualitative molecular orbital energy level diagram for a transition metal in a pseudoaxial (η^7-C_7H_7)-(η^5-C_5H_5) ligand field.

analogous levels in [Ta(η^7-C_7H_7)(η^5-C_5H_4Me)] contain a 74% d contribution.

The four electrons in the $1e_2$ MOs are key in determining the nature of the transition metal−cht bond. Figure 1 suggests that the $1e_2$ MOs are metal → carbon δ back-bonding. If these MOs are largely metal-based, then the conclusion must be that there is only a small back-bonding interaction; that is, the cht ring is functioning more as a +1 ligand (the single electron in the e_2'' MO of the free ligand has been donated to the metal). By contrast, if the $1e_2$ MOs are predominantly localized on the cht ring, the metal has largely donated three electrons to the ring, which is now best classified as carrying a −3 formal charge (the free ligand e_2'' MOs have been filled with metal electrons). Our previous experimental work suggested that neither the +1 nor the −3 formal charge extreme is a good description of the transition metal−cht bond, as the $1e_2$ MOs were found to be a mixture of metal and ligand character. We concluded that the cht ring is best described as a seven-electron donor and a trivalent ligand and that three metal electrons are required to form the metal−cht bond. In doing so, however, they retain a significant degree of metal character.

In the present work, we report the results of a systematic computational study of the bonding in [M(η^7-C_7H_7)(η^5-C_5H_5)], where M is each of the 12 members of groups 4−6. Previous computational studies of the bonding in cht complexes are scarce. In 1995 one of us published a limited study of several of the title molecules, using experimental geometries and comparatively basic density functional theory.[4] The general conclusion was that the experimental values for the metal d orbital contribution to the $1e_2$ MOs were larger than the calculated, by as much as 35% for the Ta system. In 1997, Li and Bursten reported the results of their investigations into [An(η^7-C_7H_7)$_2$] (An = Th, Pa, U, Np, Pu, and Am)[5] and found that the most important metal−ligand interactions are between the 6dδ and 5fδ atomic orbitals of the metal and the e_2'' MOs of the cht rings. The resulting δ back-bonding complex MOs involve substantial mixing between the metal and ligand orbitals: 54% metal 5f and 29% 6d in [U(η^7-C_7H_7)$_2$]. In 2002, Gagliardi and Pyykkö published a B3LYP and MP2 study of [M(η^7-N_7)(η^5-N_5)] (M = Ti, Zr, Hf, Th),[6] which are isoelectronic with our target systems and in which the metal−N_7 ring bonding was found to have a significant δ component. Interestingly, this δ interaction involves both N 2pπ and (2s+2p)σ orbitals, although no population analysis data were given.

Given the discrepancy between theory and experiment in our earlier study, and the substantial advances in density functional theory and its computational implementations over the last decade, we felt there was plenty of scope for a more detailed computational investigation. There are several reasons to address this problem computationally. First, it is of interest to test the experimental assumptions and conclusions. The experimental determination of the composition of the $1e_2$ MOs was based upon the assumption that the $1a_1$ electrons display ideal metal d cross section behavior and that the $1e_1$ electrons are purely carbon 2p, and we were keen to establish if this assumption is correct. Second, the experiment can never quantify the composition of the $1e_2$ electrons in the group 4 systems, because there is no internal reference in these compounds, i.e., no electrons in the $1a_1$ MO. Thus computation can provide data that are unobtainable experimentally. As an extension of this theme, it is now well established that there are four rows of the d-block, and we are currently undertaking an investigation of the chemistry of the transactinide (6d) elements. The first results of this program—a study of metallophilicity in [ClMPH$_3$]$_2$ [M = Cu, Ag, Au, element 111]—have been recently reported,[7] and we were keen to extend our investigations into organometallic chemistry.

Computational Details

A. General Procedures. Most calculations were performed with the Amsterdam Density Functional (ADF) program suite, version 2003.01.[8−12] Scalar relativistic corrections[13] were included via the ZORA to the Dirac equation.[14,15] The basis sets employed were taken from the ADF ZORA/TZP directory: uncontracted, Slater-type functions of primarily triple-ζ

(4) Kaltsoyannis, N. *J. Chem. Soc., Dalton Trans.* **1995**, 3727.
(5) Li, J.; Bursten, B. E. *J. Am. Chem. Soc.* **1997**, *119*, 9021.
(6) Gagliardi, L.; Pyykkö, P. *J. Phys. Chem. A* **2002**, *106*, 4690−4694.
(7) O'Grady, E.; Kaltsoyannis, N. *Phys. Chem. Chem. Phys.* **2004**, *6*, 680.
(8) *ADF2003*; Department of Theoretical Chemistry, Vrije Universiteit: Amsterdam, 2003.
(9) Baerends, E. J.; Ellis, D. E.; Ros, P. *Chem. Phys.* **1973**, *2*, 41.
(10) Versluis, L.; Ziegler, T. *J. Chem. Phys.* **1988**, *88*, 322.
(11) te Velde, G.; Baerends, E. J. *J. Comput. Phys.* **1992**, *99*, 84.
(12) Fonseca Guerra, C.; Snijders, J. G.; te Velde, G.; Baerends, E. J. *Theor. Chem. Acc.* **1998**, *99*, 391.
(13) Kaltsoyannis, N. *J. Chem. Soc., Dalton Trans.* **1997**, 1.
(14) van Lenthe, E.; van Leeuwen, R.; Baerends, E. J.; Snijders, J. G. *Int. J. Quantum Chem.* **1996**, *57*, 281.
(15) van Lenthe, E.; Snijders, J. G.; Baerends, E. J. *J. Chem. Phys.* **1996**, *105*, 6505.

quality, supplemented in the case of carbon and hydrogen by a single polarization function. The frozen core approximation was used: C(1s); Ti, V, Cr (2p); Zr, Nb, Mo (3d); Hf, Ta, W (4f); and Rf, Db, Sg (5d). The local density parametrization of Vosko, Wilk, and Nusair[16] was employed in conjunction with the BLYP[17,18] and PBE[19] gradient corrections. These functionals were chosen because the former is one of the most widely used "standard" approaches, and our experience is that the latter generally gives good agreement with experimental ionization energies for transition metal systems. The ADF numerical integration parameter was set to 5.0 in all calculations, and the energy gradient convergence criterion was set to 4.5×10^{-4} au/Å in all geometry optimizations. All calculations were performed using C_s symmetry. Spin-restricted calculations were conducted for the closed-shell mixed-ring compounds of groups 4 and 6, and spin-unrestricted calculations were conducted for the group 5 analogues, which have a single electron in the $1a_1$ MO (Figure 1). Ionization energies were calculated using the ΔSCF method. Mulliken population analyses were performed.[20]

None of our calculations have incorporated spin−orbit coupling, for the following reasons. First, although ADF can include spin−orbit coupling in single point calculations, gradients are not supported. Our experience is that in "manual" optimizations (i.e., a series of single point calculations in which geometric variables are systematically altered to produce the lowest energy structure) spin−orbit coupling has negligible effects on molecular geometries, even those containing very heavy elements. Furthermore, our principal aim in this study is to analyze the electronic structure of the target molecules at their optimized geometries, and ADF does not support wave function analysis in double-group calculations. Finally, it is unlikely that spin−orbit coupling will significantly affect the ionization energies of the valence MOs of the title systems, most of which (as we shall see) are of mainly carbon 2p character.

Several ab initio MP2 calculations have also been performed. These were conducted using the Gaussian 03 code,[21] using the 6-311G** basis sets for carbon and hydrogen, and the Stuttgart-Dresden ECPs and accompanying valence basis sets for Ti, V, and Cr,[22] and Zr, Nb, Mo, Hf, Ta, and W.[23] Default parameters were used for SCF and geometry convergence.

B. Energy Decomposition Scheme. ADF defines the molecular interaction energy as the energy difference between the molecular fragments in their final positions and at infinite separation. These molecular fragments may be individual atoms or groups of atoms, and we shall see the use of both atomic and molecular fragments in this paper (for a discussion of the use of fragments within ADF, please see ref 24). These fragments are placed at their positions within the molecule. At this point there is an electrostatic interaction between them, comprising the nucleus/nucleus, nucleus/electron, and electron/electron Coulombic interactions. This electrostatic interaction is computed from the unperturbed and superimposed charge densities of the separate fragments. Next it is ensured that the overall molecular wave function satisfies the Pauli principle. This is done by requiring that the one-electron orbitals of the combined fragments form a correct single-determinantal wave function. It is extremely unlikely, however, that this will be the case for the fragment orbitals when the fragments are simply placed at their positions within the molecule because the orbitals on the different fragments will not be orthogonal to one another. Thus the next step is to orthogonalize the occupied fragment orbitals to obtain a correct single-determinantal, antisymmetrized molecular wave function. This will result in a change in the molecular charge density, and the accompanying energy change is known as the Pauli, or exchange, repulsion. The final part of the process is to allow the fragment orbitals to relax to self-consistency. This interaction energy between the orbitals of the various fragments is defined as the electronic (or orbital) interaction within ADF and is computed using the transition state procedure first developed by Ziegler and Rauk.[25,26]

Results and Discussion

A. Geometries. Full geometry optimizations were carried out within the constraint of C_s symmetry, and the results are given in Table 1. Selected data are also collected in Figure 2, from which it may be seen that there is a pronounced "sawtooth" pattern in the calculated PBE metal−carbon bond lengths for the cp rings (Figure 2a). Thus, as a period is crossed from group 4 to group 6, the metal−C(cp) bond lengths decrease, at least for the first three rows of the transition series. The trend is not quite the same for the transactinides, for which Rf and Sg have very similar metal−C(cp) bond lengths, with that for Db being a little larger. There is a significant increase in r(M−C) between the first and second rows, after which the values remain approximately constant within a given group for the 4d and 5d elements. For group 4, the transactinide (Rf) metal−C(cp) bond length is smaller than those of the 4d and 5d systems, whereas for groups 5 and 6 the transactinide metal−C(cp) bond length is the largest in the group.

The r(M−C) data for the cht ring (Figure 2b) behave similarly to those for the cp ring, except that the transactinide values are now the largest for all three groups 4−6, and not just for the latter two groups, as was the case for the cp ring data. In general, therefore, the longest r(M−C) for both rings are found for the transactinides, more so for the cht ring than the cp. Previous computational studies of transactinide molecules differ as to the trends in bond length as the transition groups are descended. For example, for MF_2^- it has been found that r(Cu−F) < r(Au−F) < r([111]−F) < r(Ag−F).[27] Earlier studies on MH by the same workers, however, found that r([111]−H) <

(16) Vosko, S. H.; Wilk, L.; Nusair, M. *Can. J. Phys.* **1980**, *58*, 1200.
(17) Becke, A. *Phys. Rev. A* **1988**, *38*, 3098.
(18) Lee, C.; Yang, W.; Parr, R. G. *Phys. Rev. B* **1988**, *37*, 785.
(19) Perdew, J. P.; Burke, K.; Ernzerhof, M. *Phys. Rev. Lett.* **1996**, *77*, 3865.
(20) Mulliken, R. S. *J. Chem. Phys.* **1955**, *23*, 1833, 1841, 2338, 2343.
(21) Frisch, M. J.; Trucks, G. W.; Schlegel, H. B.; Scuseria, G. E.; Robb, M. A.; Cheeseman, J. R.; Montgomery, J. A., Jr.; Vreven, T.; Kudin, K. N.; Burant, J. C.; Millam, J. M.; Iyengar, S. S.; Tomasi, J.; Barone, V.; Mennucci, B.; Cossi, M.; Scalmani, G.; Rega, N.; Petersson, G. A.; Nakatsuji, H.; Hada, M.; Ehara, M.; Toyota, K.; Fukuda, R.; Hasegawa, J.; Ishida, M.; Nakajima, T.; Honda, Y.; Kitao, O.; Nakai, H.; Klene, M.; Li, X.; Knox, J. E.; Hratchian, H. P.; Cross, J. B.; Adamo, C.; Jaramillo, J.; Gomperts, R.; Stratmann, R. E.; Yazyev, O.; Austin, A. J.; Cammi, R.; Pomelli, C.; Ochterski, J. W.; Ayala, P. Y.; Morokuma, K.; Voth, G. A.; Salvador, P.; Dannenberg, J. J.; Zakrzewski, V. G.; Dapprich, S.; Daniels, A. D.; Strain, M. C.; Farkas, O.; Malick, D. K.; Rabuck, A. D.; Raghavachari, K.; Foresman, J. B.; Ortiz, J. V.; Cui, Q.; Baboul, A. G.; Clifford, S.; Cioslowski, J.; Stefanov, B. B.; Liu, G.; Liashenko, A.; Piskorz, P.; Komaromi, I.; Martin, R. L.; Fox, D. J.; Keith, T.; Al-Laham, M. A.; Peng, C. Y.; Nanayakkara, A.; Challacombe, M.; Gill, P. M. W.; Johnson, B.; Chen, W.; Wong, M. W.; Gonzalez, C.; Pople, J. A. *Gaussian 03*; Gaussian Inc.: Pittsburgh, 2003.
(22) Dolg, M.; Wedig, U.; Stoll, H.; Preuss, H. *J. Chem. Phys.* **1987**, *86*, 866.
(23) Andrae, D.; Haeussermann, U.; Dolg, M.; Stoll, H.; Preuss, H. *Theor. Chim. Acta* **1990**, *77*, 123.
(24) Baerends, E. J.; Branchadell, V.; Sodupe, M. *Chem. Phys. Lett.* **1997**, *265*, 481.
(25) Ziegler, T.; Rauk, A. *Theor. Chim. Acta* **1977**, *46*, 1.
(26) Ziegler, T.; Rauk, A. *Inorg. Chem.* **1979**, *18*, 1558.
(27) Seth, M.; Cooke, P.; Schwerdtfeger, P.; Heully, J.-L.; Pelissier, M. *Chem. Phys.* **1998**, *109*, 3935.

Table 1. Selected Geometrical Parameters from the Calculated and Experimental Structures of [M(η^7-C_7H_7)(η^5-C_5H_5)] (M = groups 4−6)

M	method	r(M−C (cp))/Å	r(M−C (cht))/Å
Ti	BLYP	2.395	2.265
	PBE	2.353	2.227
	MP2	2.282	2.209
	expt[a]	2.321	2.194
V	BLYP	2.324	2.240
	PBE	2.274	2.200
	MP2	not converged	
	expt[b]	2.230	2.250
Cr	BLYP	2.238	2.208
	PBE	2.185	2.166
	MP2	2.118	2.184
Zr	BLYP	2.574	2.408
	PBE	2.531	2.371
	MP2	2.216	2.264
Nb	BLYP	2.483	2.373
	PBE	2.435	2.333
	MP2	2.401	2.278
	expt[c]	2.315	2.390
Mo	BLYP	2.397	2.339
	PBE	2.347	2.297
	MP2	2.304	2.288
Hf	BLYP	2.555	2.394
	PBE	2.516	2.362
	MP2	2.486	2.331
Ta	BLYP	2.465	2.372
	PBE	2.423	2.335
	MP2	2.216	2.264
W	BLYP	2.390	2.348
	PBE	2.343	2.309
	MP2	2.314	2.296
Rf	BLYP	2.608	2.566
	PBE	2.416	2.382
Db	BLYP	2.532	2.434
	PBE	2.488	2.392
Sg	BLYP	not converged	
	PBE	2.415	2.381

[a] Data from ref 39. [b] Data from ref 40. [c] Data from ref 41.

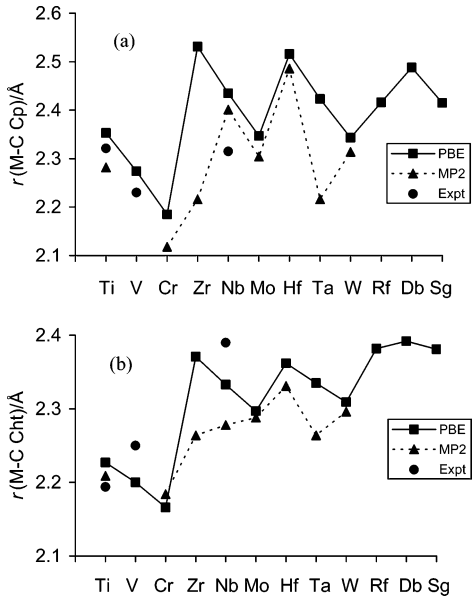

Figure 2. Calculated and experimental metal−carbon distances (Å) for (a) M−cp and (b) M−cht in [M(η^7-C_7H_7)-(η^5-C_5H_5)] (M = groups 4−6).

r(Au−H).[28] It has even been predicted that element 111 would have a smaller atomic radius than copper,[29] as a result of a pronounced actinide contraction. The present calculations suggest that there is in general no reduction in atom size between the third and fourth rows of the transition series (at least as measured by r(M−C)), suggesting that the actinide contraction is actually somewhat weaker than its lanthanide counterpart.[30]

Comparison of the PBE and BLYP data with experiment is not altogether satisfactory, although the paucity of experimental data prevents firm conclusions from being drawn. For both [Ti(η^7-C_7H_7)(η^5-C_5H_5)] and [V(η^7-C_7H_7)(η^5-C_5H_5)] the DFT calculations do a very good job of reproducing the metal−C(cp) distances (to within 0.04 Å for the PBE calculations). The discrepancy between theory and experiment for the cht rings in these compounds is also quite small (0.05 Å maximum, for [V(η^7-C_7H_7)(η^5-C_5H_5)]) although the computational reduction in r(M−C) for the cht ring between [Ti(η^7-C_7H_7)-(η^5-C_5H_5)] and [V(η^7-C_7H_7)(η^5-C_5H_5)] is in contrast to the experimentally observed increase. In the only second row system to have been experimentally characterized, [Nb(η^7-C_7H_7)(η^5-C_5H_5)], the most noticeable feature is that the calculated r(M−C) for the cht ring is smaller than experiment, while that for the cp ring is larger. We do not know why this is the case, but have conducted "lineartransit" calculations to probe the energetic consequences of altering the metal−ligand distance. These calculations are constrained geometry optimizations in which the metal−ligand distance is held fixed and the rest of the molecule allowed to optimize. For [Mo(η^7-C_7H_7)(η^5-C_5H_5)] at the PBE level (a typical calculation), shortening the metal−cp centroid distance by 0.1 Å from equilibrium carries an energetic penalty of only 14.1 kJ mol^{-1}, while lengthening this distance is unfavorable by just 4.5 kJ mol^{-1}. Equivalent data for the metal−cht centroid distance in the same molecule are 13.9 and 9.8 kJ mol^{-1}, respectively. It is therefore clear that both rings sit in rather shallow potential wells around their equilibrium positions, and this may account for the discrepancies between theory and experiment.

The r(M−C) data calculated ab initio at the MP2 level are more variable than the DFT results in that there is less of a clear pattern either across a period or down a group. The most notable differences between MP2 and DFT come at Zr and Ta, and thus there is not even a pattern as to which systems show the biggest deviations, as Zr and Ta come from different periods and groups. Perhaps the sporadic discrepancies between DFT and MP2 data are also a consequence of the flat potential wells in which the rings sit.

B. Ionization Energies. Given that the experimental data for the composition of the $1e_2$ MOs are derived from photoelectron spectroscopy, we were interested to see how our computational approach would fare when it came to calculating the principal physical observable from such experiments: ionization energies. The results of our ΔSCF calculations at the BLYP and PBE levels are collected in Table 2, together with the experimental data available for the Ti, V, Nb, Mo, and Ta systems. The ΔSCF approach involves calculating the energy difference between the neutral molecule and the molecular ion at the geometry of the neutral, i.e., assuming

(28) Seth, M.; Dolg, M.; Faegri, K.; Hess, B. A.; Kaldor, U.; Schwerdtfeger, P. *Chem. Phys. Lett.* **1996**, *250*, 461.
(29) Seth, M.; Dolg, M.; Fulde, P.; Schwerdtfeger, P. *J. Am. Chem. Soc.* **1995**, *117*, 6597.
(30) Kaltsoyannis, N.; Scott, P. *The f elements*; Oxford University Press: Oxford, 1999.

Table 2. Calculated (DFT, ΔSCF) and Experimental Ionization Energies (eV) of the Valence Molecular Orbitals of [M(η^7-C_7H_7)(η^5-C_5H_5)] (M = groups 4−6)

metal	ionizing MO (C_s)	ionizing MO (Figure 1, $C_{\infty v}$)	ion state ($C_{\infty v}$)	BLYP	PBE	expt	metal	ionizing MO (C_s)	ionizing MO (Figure 1, $C_{\infty v}$)	ion state ($C_{\infty v}$)	BLYP	PBE	expt
Ti[a]	3a″	$1e_2$	$^2E_2$	6.54	6.80	6.85	Hf	3a″	$1e_2$	$^2E_2$	6.80	7.07	
	3a′	$1e_2$		6.67	6.95			3a′	$1e_2$		6.68	6.94	
	2a″	$2e_1$	$^2E_1$	8.53	8.78	8.74		2a″	$2e_1$	$^2E_1$	8.73	9.00	
	2a′	$2e_1$		8.53	8.78			2a′	$2e_1$		8.73	9.00	
	1a″	$1e_1$	$^2E_1$	9.66	9.88	9.90		1a″	$1e_1$	$^2E_1$	9.95	10.21	
	1a′	$1e_1$		9.66	9.88			1a′	$1e_1$		9.95	10.22	
V[b]	4a′	$1a_1$	$^1A_1$	6.31	6.41	6.49	Ta[e]	4a′	$1a_1$	$^1A_1$	5.75	5.92	5.47
	3a″	$1e_2$	$^3E_2$	6.57	6.84	6.86		3a″	$1e_2$	$^3E_2$	6.85	7.12	6.89
	3a′	$1e_2$		6.57	6.85			3a′	$1e_2$		6.85	7.12	
	3a″	$1e_2$	$^1E_2$		7.13	7.35		3a″	$1e_2$	$^1E_2$		7.39	7.21
	3a′	$1e_2$			7.13			3a′	$1e_2$			7.39	
	2a″	$2e_1$	$^3E_1$	8.50	8.78	8.72		2a″	$2e_1$	$^3E_1$	8.83	9.12	8.73
	2a′	$2e_1$		8.51	8.78			2a′	$2e_1$		8.83	9.12	
	1a″	$1e_1$	$^3E_1$	9.77	10.00	10.40		1a″	$1e_1$	$^3E_1$	10.13	10.40	10.19
	1a′	$1e_1$		9.77	10.00			1a′	$1e_1$		10.14	10.41	
Cr	4a′	$1a_1$	$^2A_1$	6.29	6.42		W	4a′	$1a_1$	$^2A_1$	5.62	5.76	
	3a″	$1e_2$	$^2E_2$	7.21	7.57			3a″	$1e_2$	$^2E_2$	7.02	7.33	
	3a′	$1e_2$		7.21	7.57			3a′	$1e_2$		7.02	7.33	
	2a″	$2e_1$	$^2E_1$	8.81	9.16			2a″	$2e_1$	$^2E_1$	8.65	8.95	
	2a′	$2e_1$		8.81	9.16			2a′	$2e_1$		8.65	8.95	
	1a″	$1e_1$	$^2E_1$	10.20	10.48			1a″	$1e_1$	$^2E_1$	9.97	10.23	
	1a′	$1e_1$		10.20	10.48			1a′	$1e_1$		9.97	10.23	
Zr	3a″	$1e_2$	$^2E_2$	6.65	6.91		Rf	3a″	$1e_2$	$^2E_2$	6.59	6.83	
	3a′	$1e_2$		6.52	6.77			3a′	$1e_2$		6.47	6.69	
	2a″	$2e_1$	$^2E_1$	8.39	8.63			2a″	$2e_1$	$^2E_1$	8.39	8.63	
	2a′	$2e_1$		8.39	8.63			2a′	$2e_1$		8.39	8.63	
	1a″	$1e_1$	$^2E_1$	9.67	9.90			1a″	$1e_1$	$^2E_1$		9.85	
	1a′	$1e_1$		9.67	9.90			1a′	$1e_1$			9.85	
Nb[c]	4a′	$1a_1$	$^1A_1$	5.72	5.86	5.85	Db	4a′	$1a_1$	$^1A_1$	5.42	5.49	
	3a″	$1e_2$	$^3E_2$	6.68	6.94	7.00		3a″	$1e_2$	$^3E_2$	6.53	6.76	
	3a′	$1e_2$		6.68	6.94			3a′	$1e_2$		6.53	6.76	
	3a″	$1e_2$	$^1E_2$		7.21	7.36		3a″	$1e_2$	$^1E_2$		7.04	
	3a′	$1e_2$			7.21			3a′	$1e_2$			7.05	
	2a″	$2e_1$	$^3E_1$	8.44	8.70	8.77		2a″	$2e_1$	$^3E_1$	8.52	8.77	
	2a′	$2e_1$		8.44	8.71			2a′	$2e_1$		8.52	8.77	
	1a″	$1e_1$	$^3E_1$	9.82	10.06	10.22		1a″	$1e_1$	$^3E_1$	9.81	10.05	
	1a′	$1e_1$		9.83	10.07			1a′	$1e_1$		9.81	10.05	
Mo[d]	4a′	$1a_1$	$^2A_1$	5.81	5.94	5.70	Sg	4a′	$1a_1$	$^2A_1$	5.67	5.75	
	3a″	$1e_2$	$^2E_2$	6.27	7.39	7.38		3a″	$1e_2$	$^2E_2$	6.85	7.16	
	3a′	$1e_2$		6.27	7.39			3a′	$1e_2$		6.85	7.16	
	2a″	$2e_1$	$^2E_1$	8.49	8.79	8.86		2a″	$2e_1$	$^2E_1$	8.61	8.89	
	2a′	$2e_1$		8.49	8.79			2a′	$2e_1$		8.62	8.89	
	1a″	$1e_1$	$^2E_1$	9.94	10.20	10.38		1a″	$1e_1$	$^2E_1$	9.97	10.23	
	1a′	$1e_1$		9.94	10.20			1a′	$1e_1$		9.97	10.23	

[a] Data from ref 42. [b] Data from ref 2. [c] Data from ref 2. [d] Data from ref 3. [e] Data for [Ta(η^7-C_7H_7)(η^5-C_5H_4Me)] from ref 2.

that the formation of the molecular ion involves a vertical transition from the neutral molecule.[31] In general the PBE results are superior to the BLYP at reproducing experiment and are extremely good, with essentially quantitative agreement between theory and experiment for many of the ionizations. Calculation tends to underestimate the singlet−triplet separation in the E_2 ion states of the 17-electron group 5 systems, but only by ca. 0.1−0.2 eV. These data suggest not only that we can calculate the ionization energies of 25 atom transition metal organometallics very well but also that any differences noted above between the experimental and theoretical geometries do not have any significant effect upon the ionizations energies. They also give us confidence that our method can do equally well when applied to the composition of the valence MOs.

C. Valence Electronic Structure: Composition of the $1e_2$ MOs. As is implicit in the ionization energy data discussed above, the valence electronic structure of [M(η^7-C_7H_7)(η^5-C_5H_5)] depicted qualitatively in Figure 1 is very much supported by our calculations. As described in the Computational Details section, one of the appealing aspects of the ADF code for the present study is that it allows the breakdown of molecules into fragments, and we have chosen to analyze the composition of the valence MOs of the mixed-ring title systems in terms of contributions from the metal atom and the two carbocyclic rings. The $1e_1$ and $2e_1$ levels (each of which is an essentially isoenergetic a′ and a″ pair in C_s symmetry) are found to be largely ligand-localized (on the cht and cp rings, respectively), and the $1a_1$ MO is principally metal d in character. The $1e_2$ MOs (again, an a′ and a″ pair) are the only ones that contain a substantial contribution from both the metal and the cht ring, and these contributions (Mulliken analysis of the PBE wave function at the PBE-optimized geometry) are given graphically in Figure 3. These MOs are the only ones in the molecules to display any significant metal−ring covalency.

There is a number of interesting points in these data. First, the sum of the cht e_2'' and metal d contributions to the $1e_2$ MOs of each complex is very close to 100% in

(31) Eland, J. H. D. *Photoelectron Spectroscopy*; Butterworth: London, 1984.

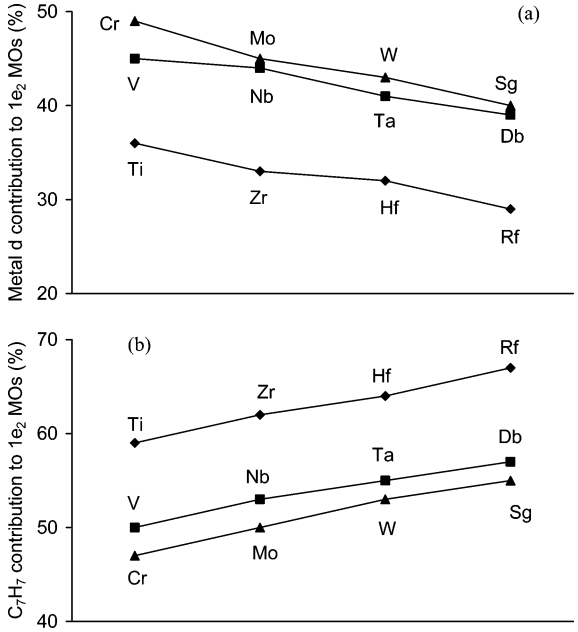

Figure 3. Calculated (a) metal d and (b) cht fragment contribution (%) to the $1e_2$ molecular orbitals (Figure 1) of [M(η^7-C_7H_7)(η^5-C_5H_5)] (M = groups 4−6).

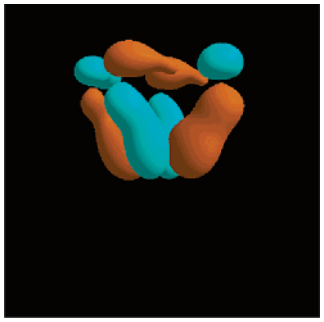

Figure 4. Three-dimensional representation of one component of the $1e_2$ molecular orbitals (Figure 1) of [Nb(η^7-C_7H_7)(η^5-C_5H_5)], generated by the ADF auxiliary program ADFview. The cht ring is situated at the top of the picture, and the Nb atom in the center.

all cases, indicating that the orbitals are indeed of the character discussed in the Introduction. In further support of this, one component of the $1e_2$ MOs of [Nb(η^7-C_7H_7)(η^5-C_5H_5)] is shown in Figure 4, beautifully illustrating the δ bond between metal and cht ring. Second, as each of the groups 4 to 6 is descended, the $1e_2$ MOs become increasingly localized on the cht ring, with a concomitant reduction in the metal d contribution. It is interesting that, while the group 5 and 6 metals in a given period have $1e_2$ MOs with similar localization properties, the group 4 analogue has $1e_2$ levels with significantly less metal d and more cht character. Given that the photoelectron spectroscopic technique used to obtain experimental data for the $1e_2$ MO composition is fundamentally incapable of providing such data for the group 4 systems, it is interesting to see that the group 4 systems are calculated to have $1e_2$ MOs with a significantly different composition from those of the group 5 and 6 molecules. We find that the compound with the most d character to the $1e_2$ MOs is [Cr(η^7-C_7H_7)(η^5-C_5H_5)], at the top of group 6, and that with the least is [Rf(η^7-C_7H_7)(η^5-C_5H_5)], at the foot of

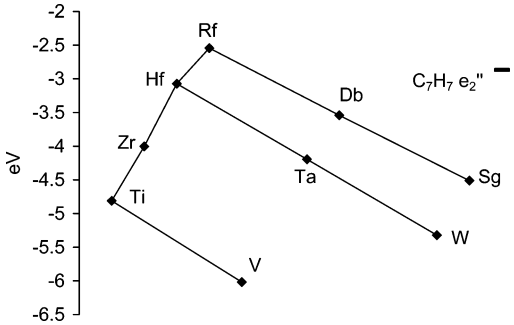

Figure 5. Calculated energies (eV) of the e_2'' molecular orbitals of cht and the d atomic orbitals of nine transition metals.

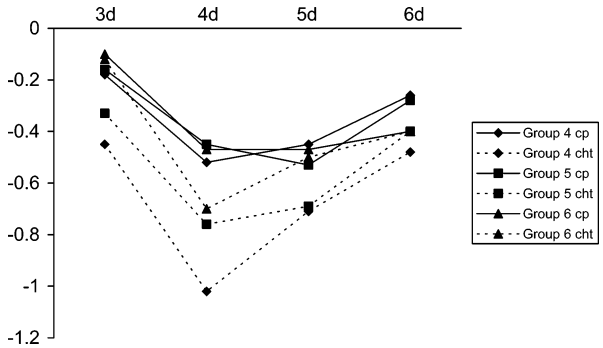

Figure 6. Calculated charges on the cht and cp rings of [M(η^7-C_7H_7)(η^5-C_5H_5)] (M = groups 4−6).

group 4. The data in Figure 3 indicate, however, that the trend from upper right to lower left in this part of the periodic table is not a uniform one, with the largest jump coming between groups 5 and 4.

It is interesting to speculate on the reason for this trend. It is likely that the relative energies of the metal d orbitals and the cht ring e_2'' levels will have a significant influence on the localization properties of the resultant complex $1e_2$ MOs. These fragment orbital energies have been calculated, and the results for cht and 9 of the 12 target metals (all those with the $d^{n-2}s^2$ atomic configuration (n = group number), as opposed to the $d^{n-1}s^1$ configuration of Cr, Nb, and Mo) are shown in Figure 5. As group 4 is descended, the metal d orbital energy becomes less negative, closer to the cht e_2'' energy. This is in agreement, at least in a qualitative sense, with the decrease in metal character to the complex $1e_2$ MOs down group 4. Similarly, as one moves across a period, the metal d orbital energy becomes more negative, moving further away from the cht e_2'' levels. This should lead to more d-localized $1e_2$ MOs, as is shown by the data in Figure 3.

The data in Figure 3 indicate that as a period is crossed from group 4 to 5 and 6, the $1e_2$ MOs become less localized on the cht ring. It might therefore be expected that the charge carried by the cht ring would decrease from groups 4 to 6, as the four electrons in the $1e_2$ MOs are less cht-like. Figure 6 plots the calculated Mulliken charge on the cp and cht rings for all 12 mixed-ring title systems. It can be seen that there is comparatively little variation from group 4 to 5 and 6 in the total charge on the cp rings (the solid lines). However, this is not the case for the charge on the cht ring (dashed lines), which, as anticipated, becomes less negative across any given period. In the group 4 compounds, the

cht ring is significantly more negative than the cp, but by the time group 6 is reached, the cht and cp rings have essentially the same charge, at least for the Cr, W, and Sg compounds. Analysis of the Hirshfeld charges of the two rings indicates that the general pattern observed in the Mulliken charges also holds for this method of assigning atomic charges.

The calculated charges on the cp and cht rings are of use in determining the formal charge on the cht ring. Given that cp is formally −1 and that the calculated charge on the cht ring is in all cases at least as or more negative than that of the cp ring in the same compound, it is logical to conclude that the formal charge of the cht ring is more negative than −1, i.e., much more toward the −3 formalism than the +1.

As discussed in the Introduction, experiment concluded that there is a 63% metal d contribution to the $1e_2$ MOs of [Nb(η^7-C_7H_7)(η^5-C_5H_5)] and [Mo(η^7-C_7H_7)-(η^5-C_5H_5)] and 74% in the equivalent MOs of [Ta(η^7-C_7H_7)(η^5-C_5H_4Me)].[3] The data in Figure 3 support experiment in finding essentially the same metal d contribution to the $1e_2$ MOs of the Nb and Mo compounds, but differ from experiment in the magnitude, just 44% for [Nb(η^7-C_7H_7)(η^5-C_5H_5)] and 45% for [Mo(η^7-C_7H_7)(η^5-C_5H_5)]. Furthermore, the Ta compound is calculated to have only 41% metal contribution to its $1e_2$ levels, more than 30% less than determined experimentally. The calculations therefore suggest that the $1e_2$ electrons are much more cht-localized than was found to be the case experimentally. Even [Cr(η^7-C_7H_7)-(η^5-C_5H_5)], the compound with the largest computed d contribution to the $1e_2$ MOs, shows only 50% metal character in this level. The computational conclusion that there is rather less d and more cht e_2'' character to the $1e_2$ complex MOs than was found experimentally is very similar to that found in our earlier, less extensive, theoretical study.[4]

It is pertinent to ask why there is such a discrepancy between theory and experiment. It is of course possible that the Mulliken population analysis method is simply getting it wrong, but there are other possibilities stemming from the analysis of the experimental data. It may be that the Gelius model does not hold well for the title compounds. This model essentially views the photoelectron cross section behavior of molecular electrons as a weighted sum of the cross sections of the atomic orbitals making up the molecular orbital from which ionization has occurred,[32,33] and is known to be less reliable when the photoelectron kinetic energy is low (i.e., close to ionization threshold). This model was used in interpreting the experimental data in ref 3, and it is possible that, in the key incident photon energy range through the p→d giant resonance region, the Gelius model is inadequate. Furthermore, as noted in the Introduction, to obtain the experimental $1e_2$ composition data, it was necessary to assume that the $1a_1$ electrons were 100% metal d in character and the $1e_1$ electrons were 100% C 2p-based. Thus the $1a_1^{-1}$ photoelectron band was assumed to exhibit ideal metal d photoelectron cross section behavior, and the $1e_1^{-1}$ band ideal C 2p cross section variations. The $1e_2$ MO composition was then

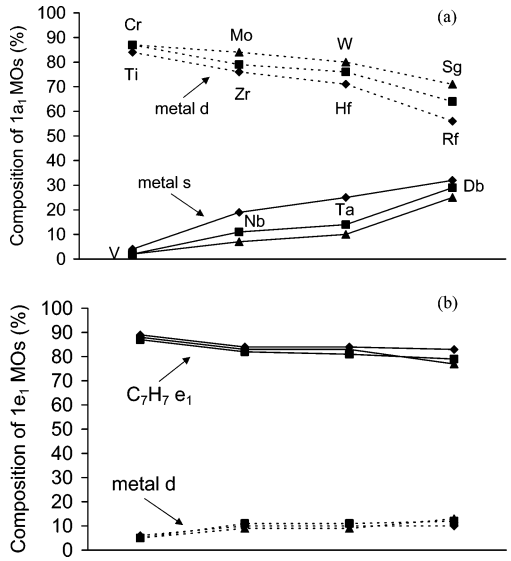

Figure 7. Calculated composition (%) of the (a) $1a_1$ and (b) $1e_1$ molecular orbitals (Figure 1) of [M(η^7-C_7H_7)-(η^5-C_5H_5)] (M = groups 4−6).

determined by comparing the variations in the $1e_2^{-1}$ band photoelectron cross section as a function of incident photon energy with those of the $1a_1^{-1}$ and $1e_1^{-1}$ bands. Figure 7 presents the calculated compositions of the $1a_1$ and $1e_1$ MOs of all 12 of the target mixed-ring systems. It shows that the $1a_1$ MOs are not 100% metal d in character (Figure 7a); indeed, for the Nb, Mo, and Ta compounds there is only ca. 80% metal d contribution to this MO. The other principal contributor is metal s. Similarly, the $1e_1$ MOs are not 100% C 2p-based, with a ca. 10% metal d contribution. It may therefore be that experiment overestimates the metal d content of the $1e_2$ MOs because the assumptions made concerning the nature of the $1a_1$ and $1e_1$ MOs are not entirely correct.

D. Strength of the Metal−cht Bond. We were interested to see how the interaction energy between the metal and the cht ring changes as a function of group and period. To this end, we decided to probe the title compounds using the energy decomposition scheme implemented in ADF (the approach is summarized in the Computational Details section and described more fully in ref 34). We chose to break the molecules down into two neutral fragments—Mcp and cht—at the PBE-optimized geometries. For the cht fragment, this choice clearly implies the electronic structure of a free cht ring, i.e., with a single electron in the e_2'' levels. We had no difficulties in obtaining this electronic structure for all of the cht fragments. The Mcp fragments, however, are rather "unchemical", and we encountered SCF convergence difficulties and needed to employ the ADF electron smearing parameter to get converged, aufbau electronic structures with integral orbital occupations. The final converged electronic structures for the group 4 Mcp fragments had three metal-based electrons, as expected: two s electrons and a d electron. For group 5 there were four metal-based electrons, and the Tacp and Dbcp fragments each had two metal s and two d

(32) Gelius, U.; Siegbahn, K. *Faraday Discuss. Chem. Soc.* **1972**, *54*, 257.
(33) Gelius, U. *Electron Spectroscopy*; North-Holland: Amsterdam, 1972.
(34) Bickelhaupt, F. M.; Baerends, E. J. In *Reviews in Computational Chemistry*; Lipkowitz, K. B., Boyd, D. B., Eds.; Wiley-VCH: New York, 2000; Vol. 15, p 1.

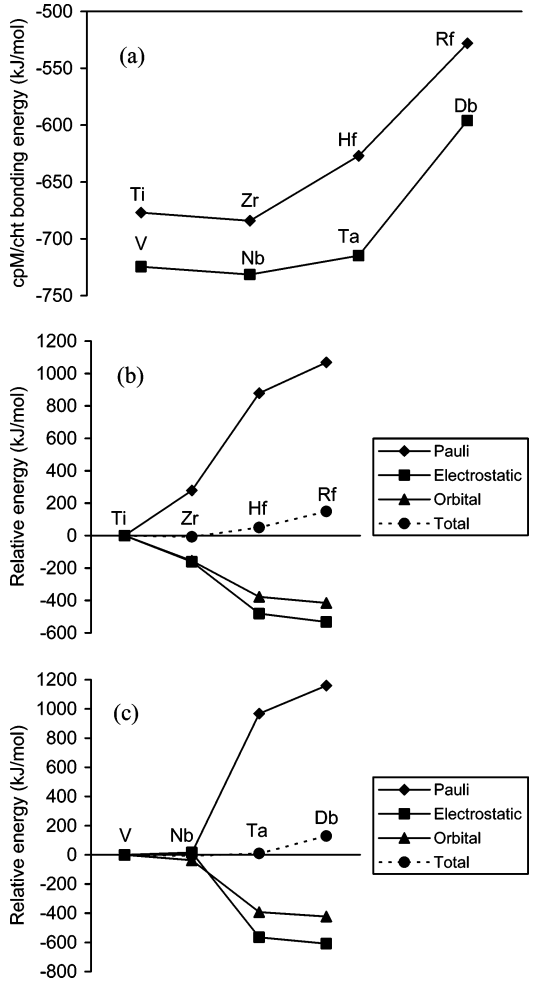

Figure 8. (a) Total cpM/cht bonding energies of [M(η^7-C_7H_7)(η^5-C_5H_5)] (M = groups 4, 5) and their breakdown into electrostatic, Pauli, and orbital contributions for (b) [M(η^7-C_7H_7)(η^5-C_5H_5)] (M = group 4) and (c) [M(η^7-C_7H_7)(η^5-C_5H_5)] (M = group 5).

electrons. For Vcp and Nbcp, there was rather more d contribution to the MO with significant metal s character than was the case for the Ta, Db, and group 4 fragments. It proved impossible to get converged electronic structures for the Mcp fragments of the group 6 metals.

The metal-based valence s orbital is not populated in the full molecules. Nevertheless, the occupation of the s orbital is necessary to achieve an aufbau electronic structure in the Mcp fragments; anything else produces an excited state. It may be that the population of this s orbital significantly affects the interaction energy between the Mcp and cht fragments, but we believe that this situation is preferable to depopulating the s orbital in the Mcp fragments and forcing them into excited states. Furthermore, the s orbital is populated in all the Mcp fragments; that is, its effects should be similar for all the molecules studied.

The interaction energies between the Mcp and cht fragments for groups 4 and 5 are shown in Figure 8a. These energies are essentially a measure of the metal−cht bond strengths, as there cannot be very much direct interaction between the two rings, and there is very little difference between the geometry of the cht and Mcp fragments in the converged molecular geometries and as free entities (i.e., there is very little fragment reorganization energy). It can be seen that the trend down the two groups is very similar, with a slight increase in bond strength from the 3d to 4d compound followed by a decrease to the third row and finally a large decrease to the transactinide system, which in both groups has a metal−cht bond more than 100 kJ mol^{-1} weaker than the 3d. The metal−cht bonds in the group 5 compounds are about 50 kJ mol^{-1} stronger than the analogous group 4 compounds, in keeping with the shorter *r*(M−C(cht)) (Figure 2b).

Figures 8b and 8c break the total bonding energy down into its electrostatic, Pauli, and orbital contributions for the group 4 and group 5 compounds, respectively. For each group, the data are normalized arbitrarily to 0 kJ mol^{-1} for the 3d compound. It is clear that the general weakening of the metal−cht bond as the groups are descended is a result of the increases in Pauli repulsion, particularly for the 5d and 6d compounds, which outweigh the favorable increases in electrostatic and orbital terms. It is possible that these large increases in the Pauli repulsion arise from the metal s orbital population in the Mcp fragments, which somehow generates a larger effect as the metals become heavier. There is also another plausible explanation, however, because as noted by Bickelhaupt and Baerends,[34] the kinetic energy component of the Pauli term (which is responsible for its overall destabilizing nature) is large in transition metal complexes when the valence orbitals of the ligands interact with the upper core levels of the metal. Clearly such an effect is dependent upon the radial extension of the upper core levels, and hence their overlap with the ligand orbitals. As the transition series is descended, the radial extension of the metals' upper core and valence orbitals becomes very similar; that is, the upper core orbitals now have significant amplitude in the outer regions of the atoms (cf. the 6p upper core orbitals in the actinides[35]), and hence the interaction of the metal's upper core levels with the ligand orbitals increases, resulting in large increases in Pauli repulsion and weaker bonds.

The trends in bond energy in the present calculations are very interesting, as it is generally the case that the strength of bonds in transition metal compounds increases as a group is descended (at least for the first three transition rows). This has been attributed to the larger radial expansion of the 4d and 5d orbitals in comparison with the 3d, and hence better overlap with the ligand functions.[36] It therefore appears that, for the 5d and 6d title systems, such increases in favorable metal−ligand orbital overlap are more than offset by the unfavorable Pauli repulsion term. As noted above, much of the largest decreases in the Mcp/cht interaction energy are found on going from the 5d to the 6d compounds. It is of course the case that there are very few data on the strength of bonds in transactinide compounds, and hence there is not yet a firm concensus. For example, the Rf−H bond dissociation energy in RfH_4 has been calculated to be significantly smaller than for the lighter group four tetrahydrides,[37] yet that for

(35) Kaltsoyannis, N. *Chem. Soc. Rev.* **2003**, *32*, 9.
(36) Tudela, D. *J. Chem. Educ.* **2000**, *77*, 1410.
(37) Pershina, V. G. *Chem. Rev.* **1996**, *96*, 1977.

Sg−CO in $Sg(CO)_6$ is predicted to be larger than for analogous W and Mo compounds.[38] We look forward to further assessing the trends in bond strength for all four members of transition groups in future studies.

Conclusions

In this contribution we have used relativistic, gradient-corrected density functional theory to investigate the geometric and electronic structures of 12 mixed-ring transition metal sandwich compounds. The principal conclusions are as follows.

1. Metal−ligand distances are generally largest for the heaviest (transactinide) members of groups 4−6.

2. Excellent agreement is obtained between calculated (ΔSCF) and previous experimental valence ionization energies.

3. The only significant covalent interaction is found in the $1e_2$ MOs. These MOs are δ bonding between the transition metal and the cht ring and are calculated to be most d-based (ca. 50%) for Cr and least d-based (ca. 30%) for Rf. These data, together with computed charges, suggest that the cht ring is functioning more as a −3 ligand than as a +1 ligand (the formal extremes). Comparison with previous experiments[3] reveals discrepancies between the two approaches with respect to the localization properties of the $1e_2$ electrons, with calculation suggesting significantly less (20−30%) d character than experiment.

4. The metal−cht bond strength is calculated to be weakest for the transactinide group 4 and group 5 systems, by >100 kJ mol^{-1} versus the 3d and 4d compounds. This is traced to increased Pauli (exchange) repulsion as groups 4 and 5 are descended.

Acknowledgment. We thank the UK Engineering and Physical Sciences Research Council for support under grants GR/S06233/01 and GR/S28020/01, and the reviewers for their helpful comments.

OM0492505

(38) Nash, C. S.; Bursten, B. E. *New J. Chem.* **1995**, *19*, 669.
(39) Zeinstra, J. D.; de Boer, J. L. *J. Organomet. Chem.* **1973**, *54*, 207.
(40) Engebreston, G.; Rundle, K. E. *J. Am. Chem. Soc.* **1963**, *85*, 481.
(41) Mawhorter, R. J.; Rankin, D. W. H.; Robertson, H. E.; Green, M. L. H.; Scott, P. *Organometallics* **1994**, *13*, 2401.
(42) Davies, C. E.; Gardiner, I. M.; Grebenik, P. D.; Green, J. C.; Green, M. L. H.; Hazel, N. J.; Mtetwa, V. S.; Prout, K. *J. Chem. Soc., Dalton Trans.* **1985**, 669.